Channel-coupling, target-structure, and second-order effects in electron-impact ionization of Ar(3*p*) and Ar(3*s*)

Klaus Bartschat and Oleg Vorov
Department of Physics and Astronomy, Drake University, Des Moines, Iowa 50311, USA
(Received 2 June 2005; published 29 August 2005)

The importance of second-order effects in the projectile-target interaction, channel coupling in the ejected-electron–residual-ion interaction, and multiconfiguration effects in the target description is investigated for electron-impact ionization of argon. For incident projectile energies of 200 and 113.5 eV, a scattering angle of 15°, and ejected-electron energies between 2 and 20 eV, we find a strong sensitivity of the theoretical predictions to the target structure, channel coupling, and the proper treatment of nonlocal exchange. In some cases, accounting for these effects seems more important than extending a local-exchange, single-configuration distorted-wave theory by including the accurate three-body Coulomb asymptotic boundary condition. Despite encouraging improvement in agreement between our predictions and recent experimental results in some cases, severe discrepancies remain in others. More experimental data, preferably absolute but at least cross-normalized to each other for a variety of kinematic conditions, seem necessary to further guide ongoing theoretical efforts.

DOI: 10.1103/PhysRevA.72.022728 PACS number(s): 34.80.Dp

I. INTRODUCTION

In recent work, Prideaux *et al.* [1] studied the effects of exchange distortion and postcollision interaction (PCI) on intermediate-energy electron-impact ionization of argon, leaving the residual ion in the $Ar^+(3s^23p^5)^2P^o$ state. An extensive list of previous work on this and closely related collision problems, such as ionization of other heavy noble gases and different final ionic states, over the past three decades can also be found in that work and will not be repeated here. Briefly, the theoretical predictions of Prideaux *et al.* [1] were obtained by three different methods, namely, (1) a standard first-order approach, in which all electrons were described by distorted waves and exchange distortion was neglected; (2) a 3DW method, in which the Coulomb interaction between the two outgoing electrons (still described by distorted waves) and therefore post-collision interaction (PCI) is accounted for to all orders of perturbation theory in the final-state wave function [2], but exchange distortion is still neglected; and (3) a hybrid method, in which the projectile-target interaction is treated by a first-order distorted-wave method while the initial state and the ejected-electron–residual-ion interaction are handled via an *R*-matrix (close-coupling) expansion. This guarantees a numerically exact treatment of exchange distortion for the slow ejected electron. Also, elaborate target wave functions were used in the latter calculation for both the initial bound state and the final ionic states. On the other hand, PCI effects were completely neglected.

Comparing their theoretical results with recent experimental data from Haynes and Lohmann [3] and Stevenson *et al.* [4], Prideaux *et al.* [1] found that including the PCI effect in their 3DW models qualitatively improved agreement with experiment over that obtained in their pure distorted-wave approach, but the neglect of exchange distortion for the slow ejected electron with energies between 2 and 20 eV was apparently too crude an approximation in many of the cases studied. Unfortunately, approximating exchange by a local potential, such as that of Furness and McCarthy [5], is known to be problematic for this case [6]. Although the agreement was far from being perfect, the hybrid method often produced superior agreement between experiment and theory, indicating that a proper treatment of exchange distortion, channel coupling, and the use of a sophisticated target description may be equally as, if not more important than, accounting for the PCI effect, at least for the kinematical situation studied in Refs. [3,4].

Ionization with the ion remaining in the $Ar^+(3s3p^6)^2S$ state was not discussed by Prideaux *et al.* [1]. However, this case was looked at earlier by Biava *et al.* [7] and by Prideaux and Madison [8]. For the two higher ejected-electron energies of 10 and 7.5 eV, the 3DW calculations in the latter paper produced very satisfactory agreement between theory and the relative experimental data of Haynes and Lohmann [9], while this was not at all the case for the two lower energies of 5 and 2 eV. Finally, comparing the distorted-wave no-exchange results of [7] with the 3DW results of [8], with or without exchange accounted for, shows at least qualitative agreement, while the distorted-wave results of [7] including exchange are very different. Clearly, the situation for this final ionic state warrants further investigation.

The goal of the present work, therefore, is to investigate potential reasons for the sensitivity of theoretical predictions for these two ionization processes. To our knowledge, all previous calculations for fully differential cross sections used distorted waves for the relatively slow ejected electron. Also, only one ionizing collision between the electron and target was accounted for. And finally, little attention has been paid to date to the quality of the target description, which typically has been limited to single-configuration expansions. Consequently, we discuss these various aspects in our theoretical model in the next section. This is followed by a comparison of our results with the recent experimental data of Haynes and Lohmann [3] and Stevenson *et al.* [4].

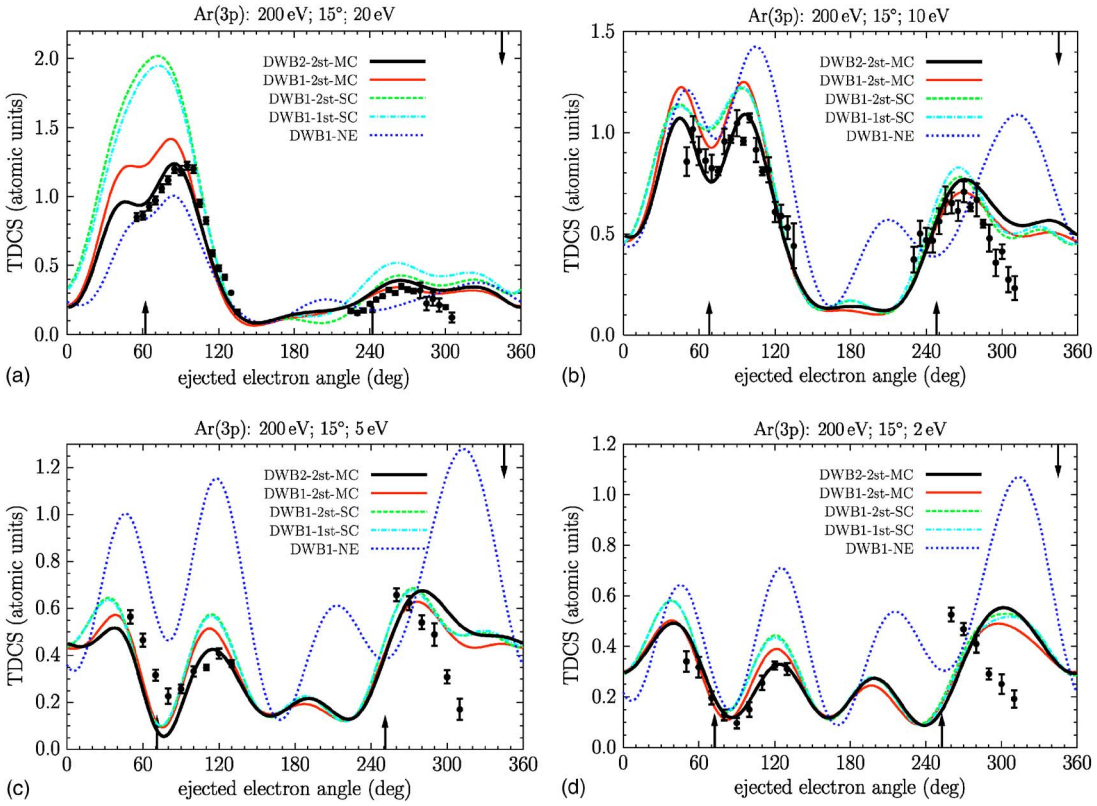

FIG. 1. (Color online) Fully differential cross sections (in atomic units) for 200 eV electron-impact ionization of the $3p$ shell of argon. All electron momenta lie in the same plane. The arrow from the top axis indicates the scattering angle (15°) at which the fast electron is observed. This corresponds to an angle of 345° in the coordinate system used for the ejected electron, whose energy is given in the title. The arrows from the bottom axis show the directions of $\pm\hat{\boldsymbol{q}}$, where $\boldsymbol{q}$ is the momentum transfer. The experimental data of Stevenson *et al.* [4] are visually normalized to the DWB2-2st-MC results in the binary region.

II. THEORY

The basic theoretical and computational method for a first-order distorted-wave treatment of the process has been outlined before [10,11], as have the extensions to account for second-order effects in the projectile-target interaction [12]. Hence we will not repeat the details here. Instead we will focus on a general discussion of the ingredients in a first-order theory and specify some details of the current model for electron-impact ionization of argon.

In our model, the first-order amplitude is given by [10]

$$f_{L_0M_0S_0M_{S_0},\mu_0\to L_fM_fS_fM_{S_f},\mu_1\mu_2}(\boldsymbol{k}_0,\boldsymbol{k}_1,\boldsymbol{k}_2) = -\frac{1}{(2\pi)^{5/2}}\langle\varphi^{(-)}_{\boldsymbol{k}_1\mu_1}(x)\Psi^{\boldsymbol{k}_2\mu_2(-)}_{L_fM_fS_fM_{S_f}}(X)|V(x,X)|\Psi_{L_0M_0S_0M_{S_0}}(X)\varphi^{(+)}_{\boldsymbol{k}_0\mu_0}(x)\rangle. \quad (1)$$

Here

$$X=\{\boldsymbol{r}_1,\sigma_1;\boldsymbol{r}_2,\sigma_2;\ldots;\boldsymbol{r}_{N+1},\sigma_{N+1}\} \quad (2)$$

denotes a set of electronic spatial and spin coordinates in the $(N+1)$-electron atom, while $x=\{\boldsymbol{r},\sigma\}$ denotes the coordinates of the colliding electron. The Coulomb potential

$$V(x,X)=\sum_{n=1}^{N+1}\frac{1}{|\boldsymbol{r}-\boldsymbol{r}_n|}-\frac{Z}{\boldsymbol{r}} \quad (3)$$

describes the interaction between the projectile and the atomic electrons as well as the nucleus. The integration in the matrix element is performed over the (x,X) coordinates of all $N+2$ electrons.

Since we use a nonrelativistic model and also neglect exchange between the "fast" projectile and the target electrons, the spin factors out via a Clebsch-Gordan coefficient [13]. In

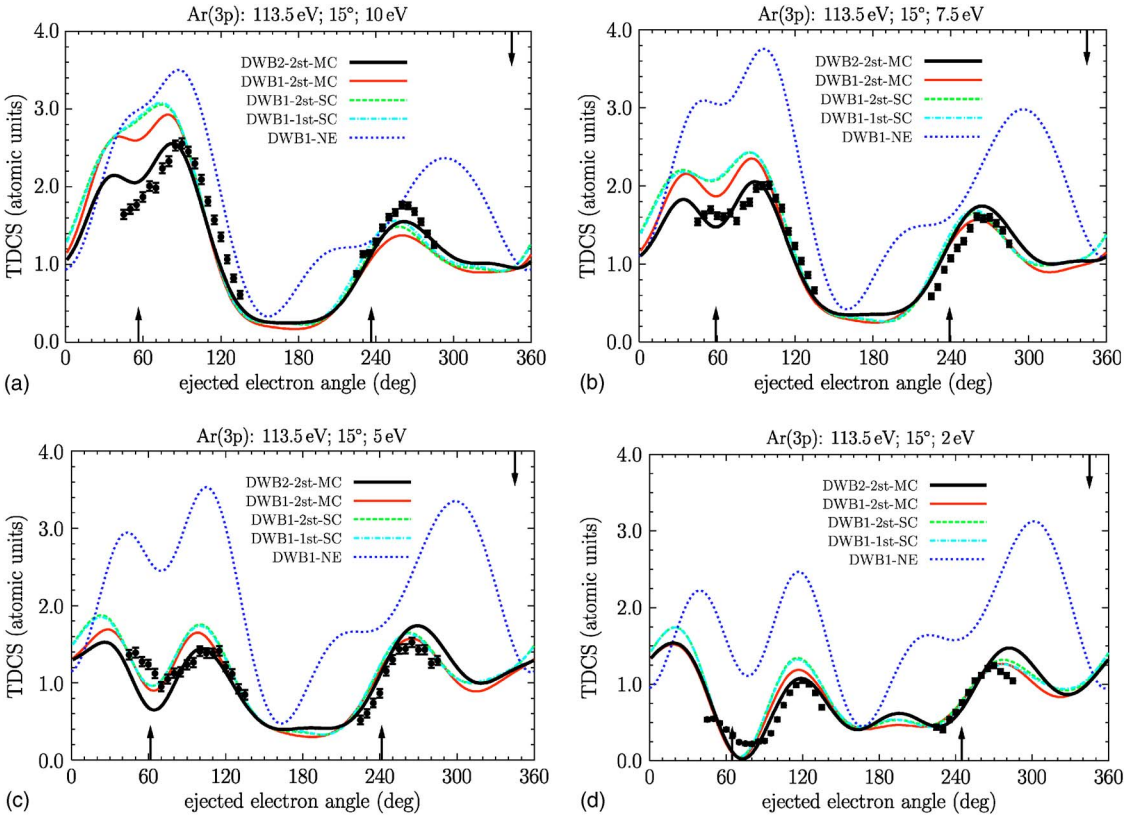

FIG. 2. (Color online) Fully differential cross sections (in atomic units) for 113.5 eV coplanar electron-impact ionization of the $3p$ shell of argon in the scattering plane. The experimental data of Haynes and Lohmann [3] are visually normalized to the DWB2-2st-MC results in the binary region.

a distorted-wave treatment for the projectile, which is critical for a target such as argon at the relatively low incident energies we will consider in this paper, we use a partial-wave description for $\varphi^{(+)}_{\boldsymbol{k}_0\mu_0}(x)$ and $\varphi^{(-)}_{\boldsymbol{k}_1\mu_1}(x)$. This actually simplifies the angular integration over the projectile coordinates in the second-order term. As noted by Reid *et al.* [12], however, we still need to make approximations to evaluate the second-order term. These include the use of only the pole term in a principal-value integral, effectively dropping the real part of the Green's function for propagating through the intermediate states, the choice of an average excitation energy for the intermediate state ("quasiclosure"), and limiting the evaluation of integrals to within the R-matrix sphere. Note that we have strong, though only indirect, evidence that these approximations are at least reasonable for ionization and simultaneous ionization-excitation of helium [14].

Another important aspect is the treatment of the ejected-electron–residual-ion interaction, i.e., the function $\Psi^{\boldsymbol{k}_2\mu_2(-)}_{L_fM_fS_fM_{S_f}}$ in Eq. (1). In principle, coupling a large number of discrete and pseudostates will ultimately lead to a converged result for the electron–residual-ion (here Ar^+) collision problem, as well as the initial bound state. This is the basic idea behind the convergent close-coupling (CCC) [15] and the R-matrix with pseudostates (RMPS) [16,17] methods.

Typical simplifications in the treatment of this part of the problem include (i) limiting the number of coupled states, and (ii) using a distorted wave for the ejected electron, with exact, approximate, or no exchange accounted for, or in the extreme case an unperturbed Coulomb wave. When checking the effect of including the three-body Coulomb boundary condition, Prideaux and Madison [8] and Prideaux *et al.* [1] effectively used a one-state model with local or no exchange for this collision problem, together with single-configuration target wave functions. With increasing projectile and ejected-electron energies, some of these approximations become less critical.

Coming back to the target description, we note that the initial bound state for a complex targets is often represented by single-configuration Hartree-Fock, multiconfiguration Hartree-Fock, or frozen-core multiconfiguration Hartree-Fock descriptions. A variant of the latter method is achieved in the R-matrix approach by running the electron-ion collision problem with modified boundary conditions to obtain the bound states of the system. In the present work, we used the multiconfiguration ionic target description given by Burke and Taylor [18] for the corresponding photoionization problem and later by Bartschat and Burke [19] in the calculation of single-differential (with respect to energy loss) and total ionization cross sections of argon by electron impact. In addition to the two-state model, in which the $Ar^+(3s^23p^5)^2P^o$ and $Ar^+(3s3p^6)^2S$ states are closely coupled, we also performed one- and five-state calculations with the orbitals and configuration expansions obtained by diagonalizing the ionic target Hamiltonian. Due to the pseudo-orbitals involved, these are not well-described physical states, but nevertheless

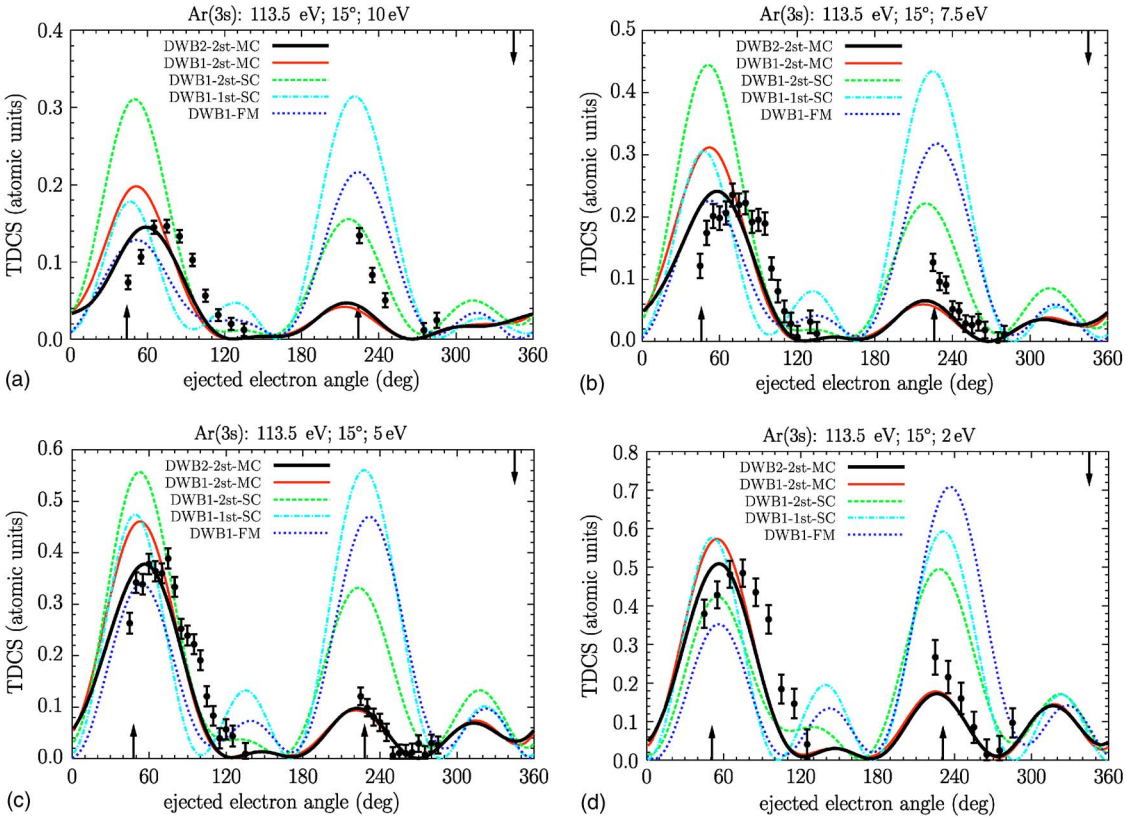

FIG. 3. (Color online) Fully differential cross sections (in atomic units) for 113.5 eV coplanar electron-impact ionization of the 3*s* shell of argon in the scattering plane. The experimental data of Haynes and Lohmann [9] are visually normalized to the DWB2-2st-MC results in the binary region.

they will give a first indication about the importance of additional channel coupling. The one-state model only included the $Ar^+(3s^23p^5)^2P^o$ state, while the five-state model added the next higher ^2S, $^2P^o$, and ^2D ionic states to the two-state approach. Finally, we also used single-configuration descriptions of the $Ar^+(3s^23p^5)^2P^o$ and $Ar^+(3s3p^6)^2S$ states and calculated a 4*s* valence orbital to include the ionic states with configurations $Ar^+(3s3p^54s)$, $Ar^+(3s^23p^44s)$, and $Ar^+(3s3p^44s^2)$. Although small configuration mixing will occur in this case between states of the same symmetry, we will refer to this as a "single-configuration" (SC) description, in order to distinguish it from the large multiconfiguration (MC) expansions that employ specially designed pseudo-orbitals to improve the target structure.

Finally, we note that fully nonperturbative approaches, such as time-dependent close-coupling [20] or exterior complex scaling [21] on a numerical grid for at least three radial coordinates could, in principle, be applied to the full problem including the fast projectile, and so could the CCC and RMPS methods. However, all of these methods require major computational resources as well as further algorithm work to handle open-shell residual ions of even limited complexity, such as $Ar^+(3p)$ and $Ar^+(3s)$. Hence, it seems unlikely that either one of these methods will be applied to the ionization of argon in the near future.

III. RESULTS

We performed many calculations, using a variety of models: First-order (DWB1) or second-order (DWB2) distorted-wave Born approximation for the fast projectile; one-, two-, five-, or ten-state (#st in the legends of the figures) close-coupling expansions for the initial state and the ejected-electron–residual-ion scattering process; and single-configuration (SC) and multi-configuration (MC) representations of the initial bound state and the final ionic states. Our results are compared below with experimental data from Stevenson *et al.* [4] for an incident projectile energy of E_0=200 eV and from Haynes and Lohmann [3,9] for E_0=113.5 eV. Also shown are distorted-wave results from Prideaux and Madison [8] and Prideaux *et al.* [1]. Note that exchange effects in the latter works were approximated by the local Furness-McCarthy [5] potential (DWB1-FM) for 3*s* ionization, while they were often neglected (DWB1-NE) for 3*p* ionization, because of apparent problems with the local-potential approximation [6,7].

Figure 1 shows fully differential cross sections (in atomic units) for 200 eV electron-impact ionization of the 3*p* shell of argon in the scattering plane. The experimental data of Stevenson *et al.* [4] are normalized by a visual fit to the DWB2-2st-MC results in the binary region and compared with predictions from our various theoretical models, as well as the DWB1 no-exchange results of Prideaux *et al.* [1]. Except for the highest ejected-electron energy of 20 eV, the results from all our models are very similar, indicating that both second-order and channel-coupling effects play a relatively small role. For the 20 eV case, the height of the binary peak is predicted to be very different in the single-configuration and multiconfiguration descriptions of the tar-

get structure. It is also worth noting that a different normalization of the experimental results could make the single-configuration models look superior to all the other theories.

The overall agreement between the predictions of our presumably best model, the DWB2-2st-MC approach, with the experimental data is satisfactory. Obvious problems emerge with decreasing ejected-electron energy for angles around 300° and above, where the experimental data are clearly decreasing with increasing ejection angle while the theoretical predictions remain almost flat. This problem may be due to the neglect of the PCI effect. Since the fast outgoing electron is observed at 345° (we use the common convention of counting the scattered-electron and the ejected-electron angles from opposites sides of the incident-beam direction), one might expect the PCI effect to become important in this angular range. Qualitatively, this expectation is supported by the 3DW results presented by Prideaux *et al.* [1], but the problems with the treatment of exchange distortion in those models did not allow for a conclusive assessment. Finally, it is interesting to note how the DWB1-NE results behave relative to the curves from our models, from lying mostly below to mostly above our predictions with decreasing energy of the ejected electron.

Figure 2 exhibits similar results for a projectile energy of 113.5 eV. This time the measurements of Haynes and Lohmann [3] are for ejected-electron energies of 10, 7.5, 5, and 2 eV, respectively. The agreement between our predictions and the relative experimental data is again satisfactory, except for emission angles of the ejected electron near the direction where the fast projectile is detected. Once again, the sensitivity of the results to changes in the numerical model is limited. However, comparison with the DWB1-NE results reinforces our conclusion that a proper account of exchange distortion for the slow electron is of critical importance.

Moving on to Fig. 3, we see a dramatic change in the model sensitivity of the theoretical results for the weak ionization channel, where the Ar^+ ion is left in the $(3s3p^6)^2S$ state. Both channel coupling and the target description strongly affect the predictions, while second-order effects remain comparatively small. Since the local-exchange potential of Furness and McCarthy [5] works reasonably well for this case [7], one would expect the DWB1-FM results to lie somewhere in the vicinity of the DWB1-1st-SC results. This is indeed the case, although the one-electron orbitals used by Prideaux and Madison were slightly different from ours. Regarding agreement between theory and experiment, we note very satisfactory agreement of the DWB2-2st-MC predictions with the experimental data for slow-electron energies of 5 and 2 eV, while the growing height of the recoil peak with increasing energy of that electron is not reproduced in the model. Depending on the normalization chosen, the one-state models in general, but particularly the DWB1-FM approach, reproduce this feature much better, especially for the case of the slow electron emerging with 10 eV.

Although second-order effects are relatively small, we exhibit in Fig. 4 the sensitivity of the DWB2 results, particularly with respect to further channel coupling. Increasing the number of coupled states from two to five with a multiconfiguration and from two to ten with a single-configuration target description does not change the results significantly. Hence, the dominant channel-coupling effect is the coupling to the dominant $(3s^23p^5)^2P^o$ ionization channel. Note that a similar result was already found by Burke and Taylor [18] for the corresponding photoionization problem. Also, Amusia and Sheinerman [22] later noticed a strong dependence on configuration-interaction effects for the angle-integrated electron-impact ionization cross section for the $3s$ shell of Ar.

Finally, looking further at the trends displayed in the theoretical curves of Fig. 4 as a function of the slow-electron energy, we generally note smaller and more systematic changes than what is seen experimentally. For example, the relative height of the experimental recoil and binary peaks is smallest at 5 eV. Also, the recoil peak is bigger at 10 than at 2 eV. In the individual theoretical results for each model, on the other hand, the recoil peak is either higher or lower than the binary peak for essentially all energies of the slow electron. When the recoil peak is higher than the binary peak, as is the case in the DWB2-1st-SC model, the binary peak is slowly growing while the recoil peak is decreasing with decreasing slow-ejected electron energy. For all the other models, the trend is exactly opposite, except for the DWB2-10st-SC model, which predicts nearly equal heights of the binary and recoil peaks when the slow electron has an energy of 2 eV.

IV. CONCLUSIONS

We have investigated the importance of second-order effects in the projectile-target interaction, channel coupling in the ejected-electron–residual-ion interaction, and multiconfiguration effects in the description of the initial bound state and the final ionic states in electron-impact excitation of argon, leaving the residual ion in the $Ar^+(3s^23p^5)^2P^o$ and $Ar^+(3s3p^6)^2S$ states, respectively. For the kinematical situations considered here, incident energies of 200 and 113.5 eV, a fast-electron detection angle of 15°, and slow-electron energies between 2 and 20 eV, we found that second-order effects are generally small. This may not be too surprising, since both processes can already occur in first order with uncorrelated target wave functions.

For $3p$ ionization, specifically, channel-coupling and multiconfiguration effects in the structure description are of limited importance. On the other hand, exchange effects need to be treated properly, and using a local exchange potential is known to be problematic for this case. For $3s$ ionization, the situation is essentially reversed. A local approximation for the exchange effects is reasonable, but accounting for channel-coupling and multiconfiguration effects in the structure description is of critical importance. In particular, coupling between the $3s$ and $3p$ ionization channels cannot be neglected for the kinematics studied in the experiment [3].

In summary, the present investigation explains to a large extent why, for the kinematics investigated in the most recent experiments of Refs. 3 and 4, adding the three-body Coulomb boundary condition to a local-exchange, single-configuration distorted-wave theory did not yield substantial and consistent improvement in the agreement between ex-

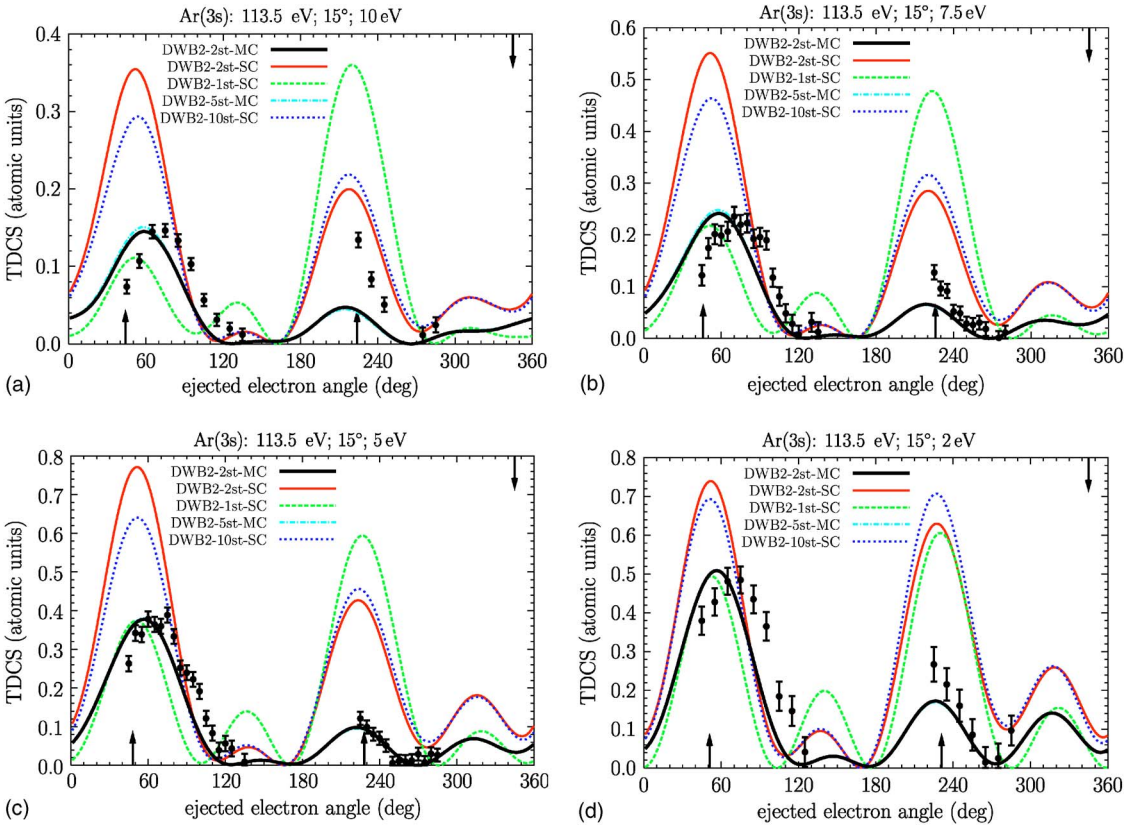

FIG. 4. (Color online) Fully differential cross sections (in atomic units) for 113.5 eV coplanar electron-impact ionization of the 3*s* shell of argon in the scattering plane. The experimental data of Haynes and Lohmann [9] are visually normalized to the DWB2-2st-MC results in the binary region. Note that the DWB2-2st-MC and DWB2-5st-MC curves are barely distinguishable.

periment and theory. Unfortunately, the present method does not always achieve good agreement with experiment either. Interestingly, some of the trends seen in the limited amount of experimental data are not as smooth a function of the ejected-electron energy as those seen in the theoretical predictions. It is clear that more experiments are required to guide further theoretical efforts. While these data sets should preferably be absolute, relative results for different kinematics should definitely be *cross-normalized* to each other, in order to better assess the strengths and weaknesses of current theoretical approaches. It would be highly desirable to develop a method that can account for all the effects discussed in the present work, as well as the postcollision interaction.

ACKNOWLEDGMENTS

The authors would like to thank Albert Crowe, Birgit Lohmann, Don Madison, and Alexei Grum-Grzhimailo for helpful discussions. This work was supported by the United States National Science Foundation under Grant No. PHY-0244470.

[1] A. Prideaux, D. H. Madison, and K. Bartschat (unpublished).
[2] M. Brauner, J. S. Briggs, and H. Klar, J. Phys. B **22**, 2265 (1989).
[3] M. A. Haynes and B. Lohmann, Phys. Rev. A **64**, 044701 (2001).
[4] M. Stevenson, G. J. Leighton, A. Crowe, K. Bartschat, O. K. Vorov, and D. H. Madison, J. Phys. B **38**, 433 (2005).
[5] J. B. Furness and I. E. McCarthy, J. Phys. B **6**, 2280 (1973).
[6] D. A. Biava, K. Bartschat, H. P. Saha, and D. H. Madison, J. Phys. B **35**, 5121 (2002).
[7] D. A. Biava, H. P. Saha, E. Engel, R. M. Dreizler, R. P. McEachran, M. A. Haynes, B. Lohmann, C. T. Whelan, and D. H. Madison, J. Phys. B **35**, 293 (2002).
[8] A. Prideaux and D. H. Madison, Phys. Rev. A **67**, 052710 (2003).
[9] M. A. Haynes and B. Lohmann, J. Phys. B **33**, 4711 (2000).
[10] K. Bartschat and P. G. Burke, J. Phys. B **20**, 3191 (1987).
[11] K. Bartschat, Comput. Phys. Commun. **75**, 219 (1993).
[12] R. H. G. Reid, K. Bartschat, and A. Raeker, J. Phys. B **31**, 563 (1998); **33**, 5261 (2000).
[13] K. Bartschat and A. N. Grum-Grzhimailo, J. Phys. B **35**, 5035 (2002).
[14] Y. Fang and K. Bartschat, J. Phys. B **34**, L19 (2001).
[15] I. Bray, D. V. Fursa, A. Kheifets, and A. T. Stelbovics, J. Phys.

B **35**, R117 (2002).
[16] K. Bartschat, E. T. Hudson, M. P. Scott, P. G. Burke, and V. M. Burke, J. Phys. B **29**, 115 (1996).
[17] K. Bartschat, Comput. Phys. Commun. **114**, 168 (1998).
[18] P. G. Burke and K. T. Taylor, J. Phys. B **8**, 2620 (1975).
[19] K. Bartschat and P. G. Burke, J. Phys. B **21**, 2969 (1988).
[20] M. S. Pindzola, F. J. Robicheaux, J. P. Colgan, M. C. Witthoeft, and J. A. Ludlow, Phys. Rev. A **70**, 032705 (2004).
[21] C. W. McCurdy, D. A. Horner, and T. N. Rescigno, Phys. Rev. A **65**, 042714 (2002).
[22] M. Ya. Amusia and S. A. Sheinerman, J. Phys. B **12**, 649 (1979).